Rotational wavepacket dynamics of the C_{60} molecule

J. Phys. B: At. Mol. Opt. Phys. **33** (2000) 1663–1674. Printed in the UK PII: S0953-4075(00)50194-1

Rotational wavepacket dynamics of the C_{60} molecule

I Jex†‡ and G Alber†

† Abteilung Quantenoptik, Universität Ulm, Albert-Einstein-Allee 11, D-89069 Ulm, Germany
‡ Department of Physics FJFI ČVUT, Břehová 7, 115 19 Praha 1, Staré Město, Czech Republic

Received 7 February 2000

Abstract. The wavepacket dynamics of (non-stationary) rotational quantum states of the C_{60} molecule are investigated. It is demonstrated that the icosahedral symmetry of this molecule gives rise to a variety of peculiar coherence phenomena which are characteristic for this specific discrete symmetry group. On the one hand, the dynamics of these wavepackets reflects the underlying classical dynamics on the associated manifold of group space. On the other hand, these dynamics also exhibit characteristic quantum features such as the appearance of fractional revivals, of quantum tunnelling between different classically accessible regions of the associated manifold of group space and of cat-like quantum states which are generated in the course of the time evolution.

(Some figures in this article are in colour only in the electronic version; see `www.iop.org`)

1. Introduction

Recent progress in the generation and manipulation of single atoms and molecules has opened up new possibilities for studying basic properties of matter in new parameter regimes. The numerous experiments which have been performed so far on the dynamics of atoms in standing-wave light fields [1] suggest that the diffraction of molecules by electromagnetic fields might offer interesting new perspectives due to the expected intricate interplay between internal and external degrees of freedom. In this context fullerenes and their most famous representative, namely the molecule C_{60}, constitute interesting examples [2]. Indeed, in a very recent experiment [3] wave properties have also been observed in the diffraction of a C_{60} molecule.

The molecule C_{60} is a fascinating object worthy of independent study before asking questions concerning the dynamics of this molecule in external electromagnetic fields. On the one hand, this molecule is sufficiently complex to exhibit a rich variety of quantum phenomena which are also specific for other large molecules. On the other hand, it is also amenable to a rather systematic theoretical description due to its high symmetry. Due to rapid experimental advances in the field of molecular spectroscopy the controlled preparation of coherent superpositions of rotational or vibrational states of the C_{60} molecule seems feasible in the near future so that the experimental exploration of these quantum phenomena is within reach.

Motivated by these experimental developments, in this paper the coherent dynamics of the rotational degrees of freedom of a C_{60} molecule in its electronic and vibrational ground state are investigated theoretically. Due to the icosahedral symmetry of the electronic and vibrational ground state the dynamics of these rotational degrees of freedom exhibit a rich variety of

0953-4075/00/081663+12$30.00

quantum coherence phenomena which are specific for this particular high symmetry. So far theoretical investigations in this context have concentrated mainly on the resulting structure of the rotational energy spectra which exhibit characteristic fine and superfine splittings [4]. Contrary to these previous time-independent investigations the main emphasis of this paper is on novel time-dependent effects which manifest themselves in the dynamics of rotational wavepackets. It is demonstrated that for sufficiently short times many aspects of this wavepacket dynamics can be understood on the basis of the underlying classical dynamics of the rotational degrees of freedom. These classical dynamics take place on a two-dimensional curved, compact manifold which is associated with the group space of the rotation group. For longer interaction times the dynamics of these wavepackets is dominated by characteristic coherence phenomena such as the appearance of fractional revivals and of quantum mechanical tunnelling between various classically accessible regions. Another striking feature of the long-time dynamics of these wavepackets is the appearance of cat-like states which are localized on different parts of the classical manifold of group space and which reflect the icosahedral symmetry of this molecule. The systematic exploration of these time-dependent effects might be viewed as a first, necessary step towards the final goal of obtaining a complete understanding of the more elaborate problem of coherent diffraction of rotationally excited fullerenes by a spatially varying electromagnetic field.

This paper is organized as follows. The basic Hamiltonian describing the quantum dynamics of the rotational degrees of freedom of C_{60} together with its associated classical Hamiltonian is introduced and discussed in section 2. In section 3 the time evolution of coherent states is investigated. These coherent states are well localized in the classical phase space which is associated with the classical dynamics of the rotational degrees of freedom and which forms a 2-sphere.

2. The Hamiltonian

In the ground state the molecule C_{60} forms an object having icosahedral symmetry [2]. Thus the dynamics of the rotational degrees of freedom in the electronic and vibrational ground state can be described phenomenologically by a Hamiltonian of the form [4, 5]

$$\hat{H} = B\hat{\boldsymbol{J}}^2 + T^{[6]}. \tag{1}$$

The first term of this Hamiltonian describes the dynamics of a rigid spherical top with structure constant B. The second term results from the icosahedral symmetry of the molecule and contains the invariant sixth-rank tensor

$$T^{[6]} = \tfrac{1}{5}\sqrt{11}T_0^6 + \tfrac{1}{5}\sqrt{7}(T_5^6 - T_{-5}^6). \tag{2}$$

It is formed by components of the angular momentum operator $\hat{\boldsymbol{J}}$ in the body-fixed frame of the molecule. The quantities T_q^k denote the components of an irreducible tensor of rank k with respect to the rotation group [6]. Their matrix elements with respect to the angular momentum eigenstates $|J, m\rangle$ in the body-fixed frame of the molecule, i.e. $\hat{\boldsymbol{J}}_3|J, m\rangle = m|J, m\rangle$, $\hat{\boldsymbol{J}}^2|J, m\rangle = J(J+1)|J, m\rangle$ (where J and m are integers), can be obtained with the help of the Wigner–Eckart theorem [6]. Within a given J-manifold these matrix elements can be expressed in terms of Wigner $3j$ symbols [6] by

$$\langle J, m|T_q^6|J, m'\rangle = (-1)^{J-m}\sqrt{2J+1}\begin{pmatrix} 6 & J & J \\ q & m & -m' \end{pmatrix}\langle J\|T^{[6]}\|J\rangle. \tag{3}$$

Thereby the reduced matrix element $\langle J\|T^{[6]}\|J\rangle$ depends only on the value of the angular momentum J.

The sixth-rank tensor of equation (2) is the invariant of lowest non-trivial order with icosahedral symmetry. The invariant of next higher order in the angular momentum operators $\hat{\boldsymbol{J}}$ is of order ten and we assume that its contribution to the dynamics is negligible. The order of this non-trivial tensorial invariant can be derived in a straightforward way from the character table of the icosahedral symmetry group [4]. Thus apart from the spherical top contribution the Hamiltonian of equation (2) might be viewed as arising from a power-series expansion in terms of the angular momentum operator $\hat{\boldsymbol{J}}$ of the molecule in which only the term of lowest order is kept, which is invariant under the icosahedral symmetry group. Within this approach the rotational dynamics of a C_{60} molecule is characterized by the two structure constants B and $\langle J \| T^{[6]} \| J \rangle$. In the subsequent discussion it will be assumed that the contribution of the tensorial invariant of sixth order is much smaller than the leading term describing a spherical top. Thus the influence of this sixth-order tensorial invariant can be treated perturbatively and causes a small splitting of each J-manifold of the spherical top into a icosahedral multiplet. It should be mentioned that contributions higher than second order in $\boldsymbol{J}$ which are spherically symmetric have been neglected in the Hamiltonian of equation (1). Within a perturbative treatment these terms would give rise to global level shifts of each J-manifold of the spherical top which do not affect the relative energy positions within each icosahedral multiplet.

The typical structure of such a multiplet, which has already been analysed in detail previously [4], is plotted in figure 1 for $J = 300$. The eigenvalues within each multiplet form clusters of almost degenerate eigenvalues. The small splittings between these energy levels within one of these clusters are called superfine-structure splittings [4, 5]. Within a semiclassical description of the rotational dynamics this superfine splitting might be traced back to effects of quantum mechanical tunnelling between trajectories of the corresponding

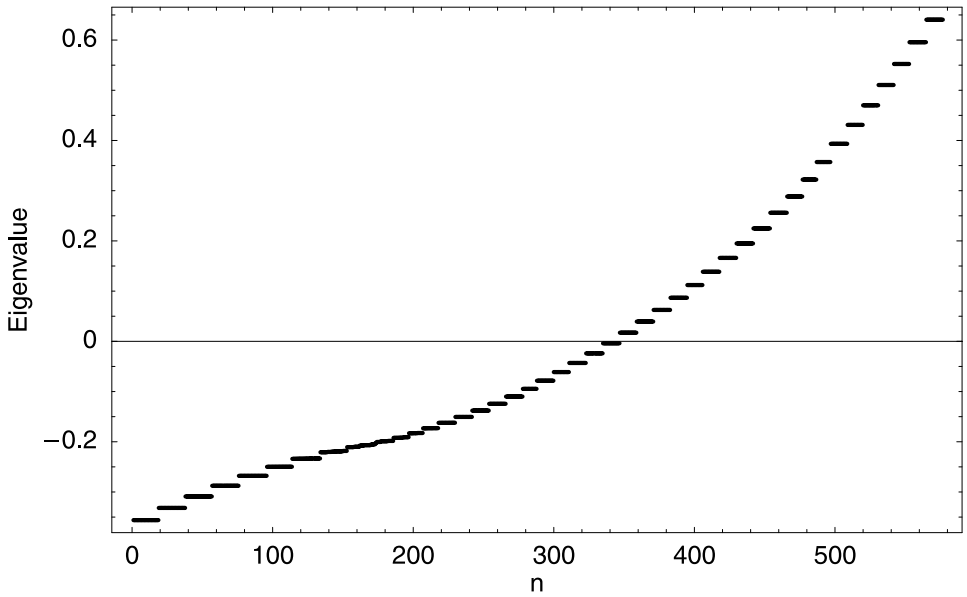

Figure 1. Eigenvalues of the rescaled Hamiltonian $\tilde{H} = (H - B\hat{J}^2)/(\langle J \| T^{[6]} \| J \rangle)$ calculated for $J = 300$. The minimum (maximum) eigenvalue approaches the classical limit of $E = -\sqrt{11}/9$ ($E = \sqrt{11}/5$). The thickness of the lines is used to indicate the superfine structure of the spectrum. Note the high energy density near the classical separatrix energy $E = -\sqrt{11}/16$.

classical dynamics. In this example the orders of magnitudes of these splittings range from 10^{-3} for the lowest-lying states up to 10^{-7} for the highest excited states within the multiplet (in units of $\langle J\|T^{[6]}\|J\rangle$). The fine structure of this multiplet, i.e. the energy separation between different clusters, is much larger in magnitude and it originates from the breaking of the spherical symmetry by the icosahedral structure of the molecule. One also notes that there is an energy region of a particularly high level density. In a classical description of the rotational dynamics this energy regime corresponds to classical separatrix motion.

In order to obtain some more insight into the classical aspects of the rotational dynamics which underlie these energy splittings let us consider the classical Hamiltonian associated with equation (1), namely

$$\mathcal{H} = BJ^2 + C\tfrac{1}{80}\sqrt{11}\big(231\cos^6\beta - 315\cos^4\beta + 105\cos^2\beta - 5 \\ +42\cos\beta\sin^5\beta\cos(5\phi)\big)J^6. \tag{4}$$

This Hamiltonian involves the Cartesian angular momentum components

$$\begin{aligned} J_{\bar{x}} &= J\sin(-\beta)\cos(-\phi) \\ J_{\bar{y}} &= J\sin(-\beta)\sin(-\phi) \\ J_{\bar{z}} &= J\cos(-\beta) \end{aligned} \tag{5}$$

in the body-fixed frame of the molecule. The angles $(-\beta)$ and $(-\phi)$ denote the associated polar and azimuthal angles in the molecular body-fixed frame [4]. This Hamiltonian is symmetric with respect to the icosahedral symmetry group. Analogously to equation (1), it is constructed from the Hamiltonian of the spherical top and from the lowest-order polynomial of the angular momentum components (in the body-fixed frame of the molecule) which is symmetric with respect to the icosahedral symmetry group. In equation (4) we have introduced the as yet unknown structure constant C whose value is fixed later.

In figure 2 the energy surface is depicted as a function of the Cartesian components $J_{\bar{x}}$, $J_{\bar{y}}$, $J_{\bar{z}}$ and as a function of the polar angle β and the azimuthal angle ϕ. The energy surface of the Hamiltonian of equation (4) has three types of local extrema which are defined by the conditions

$$\frac{\partial\mathcal{H}}{\partial\beta} = 0 \qquad \frac{\partial\mathcal{H}}{\partial\phi} = 0. \tag{6}$$

There are 20 degenerate minima the energies of which are given by

$$\mathcal{H}_{\min} = BJ^2 - C\tfrac{1}{9}\sqrt{11}J^6. \tag{7}$$

The separatrix energy of the 30 degenerate saddle points on the energy surface has the value

$$\mathcal{H}_{\mathrm{sep}} = BJ^2 - C\tfrac{1}{16}\sqrt{11}J^6. \tag{8}$$

The 12 degenerate maxima of the energy surface all have the value

$$\mathcal{H}_{\max} = BJ^2 + C\tfrac{1}{5}\sqrt{11}J^6. \tag{9}$$

These extremal values are apparent in the cut of the energy surface illustrated in figure 2(*c*). Identifying $CJ^6 \equiv \langle J\|T^{[6]}\|J\rangle$, the maximum value of the classical Hamiltonian of equation (4) converges to the corresponding highest energy level of the icosahedral multiplet of equation (1) for $J \gg 1$. Thus the quantum mechanical multiplets are all located inside the interval $[\mathcal{H}_{\min}, \mathcal{H}_{\max}]$. According to equation (1) for $J = 60$, for example, the highest eigenvalues of the Hamiltonian $(\hat{H} - B\hat{\boldsymbol{J}}^2)/\langle J\|T^{[6]}\|J\rangle$ equal 0.5576, while the smallest eigenvalues are given by -0.3319. For $J = 300$, for example, the corresponding maximum and minimum values are given by 0.640 and -0.356, which compare well with the corresponding classical values of $\sqrt{11}/5 \approx 0.663\,324$ and $-\sqrt{11}/9 \approx -0.368\,514$.

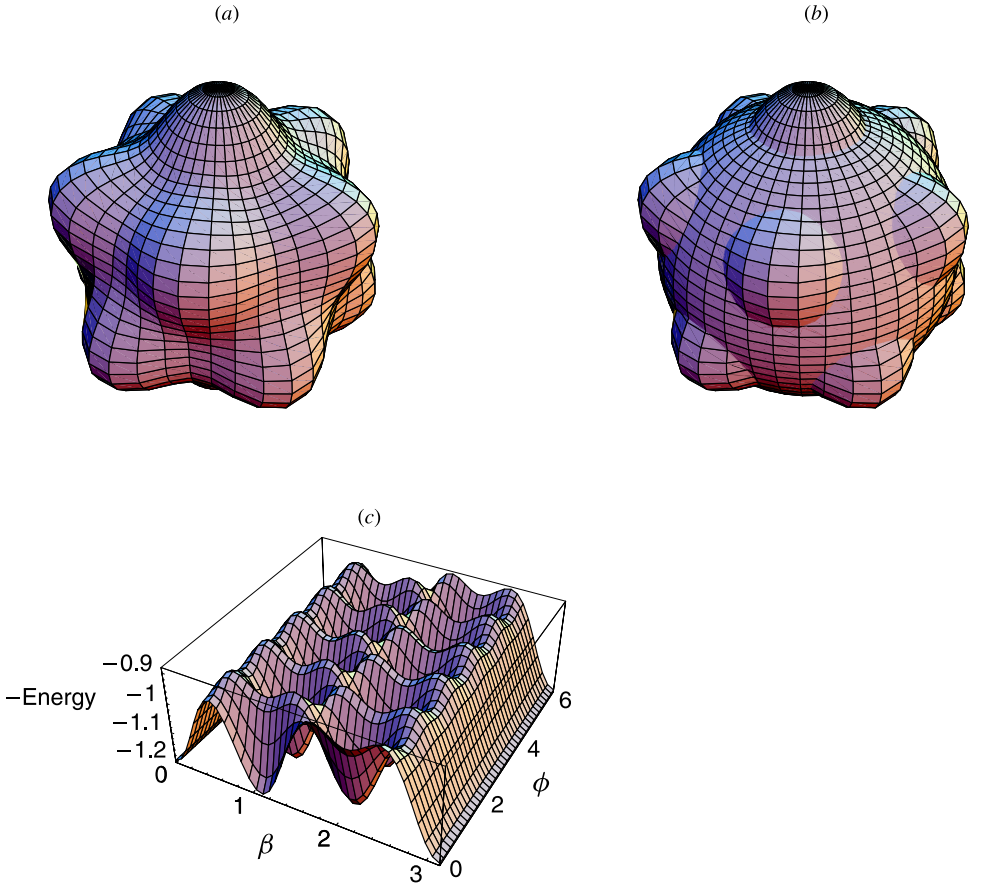

Figure 2. (*a*) Visualization of the dependence of the classical rotational energy $\mathcal{H}$ as given by equation (4) on the components of the angular momentum in the body-fixed frame of the molecule; the surface reflects the icosahedral symmetry of the molecule. The parameters are $B|J|^2 = 1$ and $CJ^6 \equiv \langle J\|T^{[6]}\|J\rangle = 0.3$. (*b*) Cut of this surface with a surface of constant energy; the resulting classical trajectories are circles. (*c*) Energy dependence of the energy surface as a function of the angles β and ϕ. To visualize the minima we plot the negative of the potential.

The possible classical motions of the body-fixed angular momentum components are obtained from the conservation of energy and angular momentum, i.e. $\mathcal{H}$ = constant and J = constant. The icosahedral symmetry of the energy surface implies that close to the maximum energy there are 12 closed classical trajectories, whereas close to the minimum energy their number increases to 20. On a semiclassical level the superfine-structure splitting might be attributed to quantum mechanical tunnelling between these energetically degenerate classical trajectories. The associated exponential dependence of these splittings on the associated imaginary actions explains the extremely small magnitudes of these superfine-structure splittings on a qualitative level. The energy barriers which have to be overcome in these tunnelling processes are higher for classical trajectories close to the maximum energy $\mathcal{H}_{\max}$ than for those close to the minimum energy $\mathcal{H}_{\min}$. This qualitative picture also explains why the superfine-structure splitting is significantly smaller for energy levels close to the maximum energy of an icosahedral multiplet than for energies close to the minimum energy. At the separatrix energy the possible classical trajectories form a closed network of paths

extending over the energy surface. This network consists of 30 unstable fixed points which are connected by classical trajectories forming a system of separatrices. Classically it takes infinite time to traverse one of these trajectories which connects an unstable and a stable manifold of two adjacent saddle points.

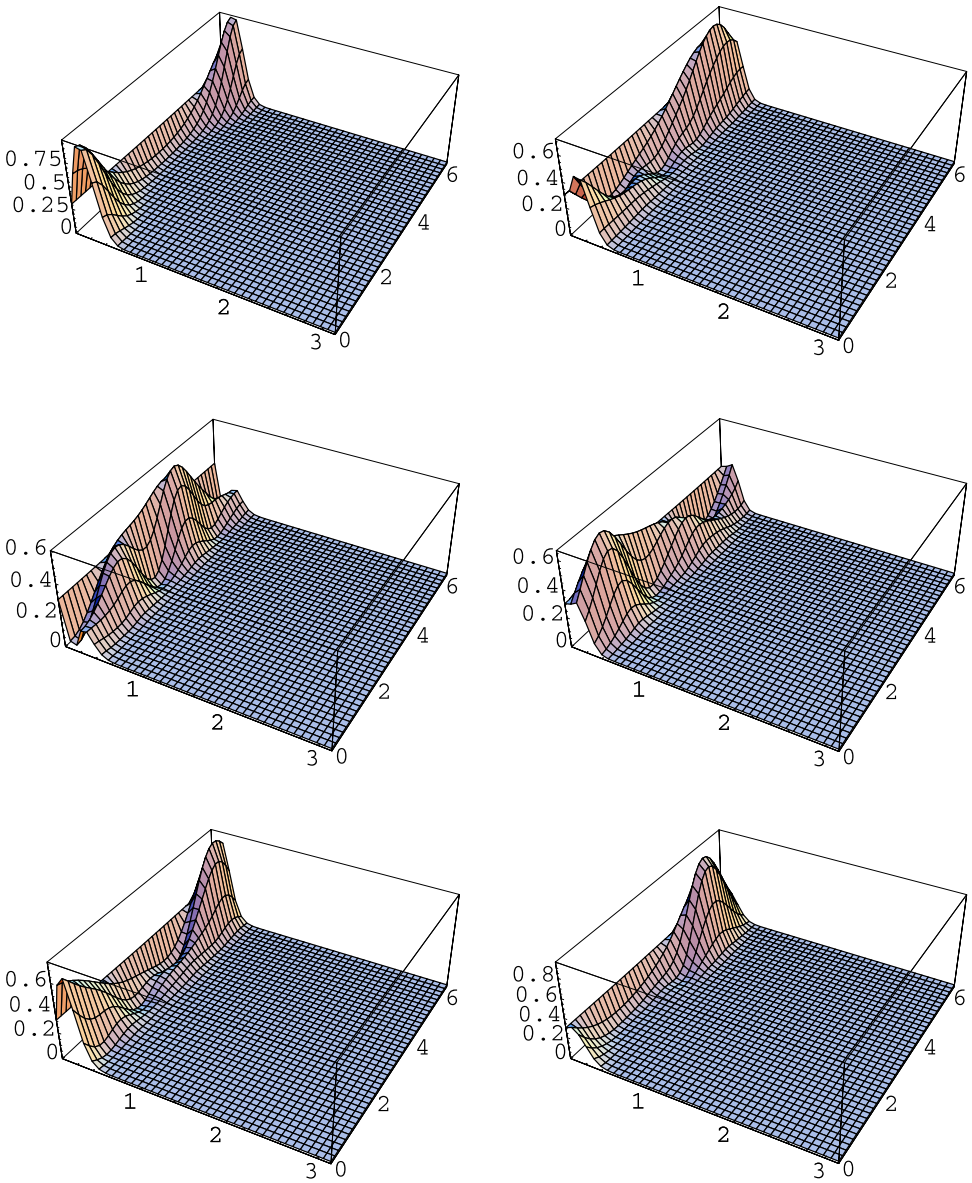

Figure 3. Time evolution of the Q-function for the coherent state $|\beta = 0.199, \phi = 0\rangle$: time steps in units of $t = 40\hbar/\langle J\|T^{[6]}\|J\rangle$. The plots are ordered from left to right and from top to bottom.

3. Rotational wavepacket dynamics—numerical examples

In this section characteristic aspects of rotational wavepackets are investigated, the dynamics of which are governed by the Hamiltonian of equation (1).

Let us assume that initially the C_{60} molecule is prepared in its electronic and vibrational ground state and that the initial rotational state is a coherent state [7] of the form

$$|\psi_{\mathrm{in}}\rangle = |\beta, \phi\rangle = \frac{1}{(1+|\tau|^2)^J} \mathrm{e}^{\tau \hat{J}^+} |J, -J\rangle = \sum_{m=-J}^{J} \sqrt{\binom{2J}{J+m}} \frac{(\tan(\beta/2)\,\mathrm{e}^{-\mathrm{i}\phi})^{J+m}}{(1+\tan(\beta/2)^2)^J} |J, m\rangle \tag{10}$$

with $\tau = \tan(\beta/2)\,\mathrm{e}^{-\mathrm{i}\phi}$. This coherent state may be visualized as being localized on a 2-sphere representing the phase space of the rotational degrees of freedom. This phase space is parametrized by the azimuthal and polar angles β and ϕ which form coordinates on this 2-sphere and which have already been introduced in section 2 (compare with equation (4)). Extreme cases of these coherent states correspond to the positions $\beta = 0$ and π, which are associated with the states $|J, -J\rangle$ and $|J, J\rangle$, respectively.

How can one prepare a coherent state of the type of equation (10)? This aim may be achieved in two steps. First, one prepares one of the states $|J, J\rangle$ or $|J, -J\rangle$. These states may be prepared with the help of a static magnetic field which is strong enough to induce Zeeman splitting in a particular J-manifold of rotational states and by selecting from the resulting Zeeman manifold the state of highest or lowest energy. Afterwards coherent states of the form of equation (10) may be prepared by inducing a rotation within this Zeeman manifold with the help of an appropriately applied additional magnetic field. During these preparatory steps the applied magnetic fields should be so strong that the influence of the icosahedral interaction Hamiltonian of equation (2) is negligible.

After its preparation the dynamics of such a coherent state are determined by the Hamiltonian of equation (1). These dynamics can be visualized conveniently with the help of the Q-function [8]

$$Q(\beta, \phi, t) = \frac{2J+1}{4\pi} |\langle \beta, \phi | \psi(t) \rangle|^2. \tag{11}$$

Thereby $|\psi(t)\rangle$ denotes the state of the system at time t. This Q-function is particularly convenient for exhibiting the relation between the quantum dynamics of the rotational

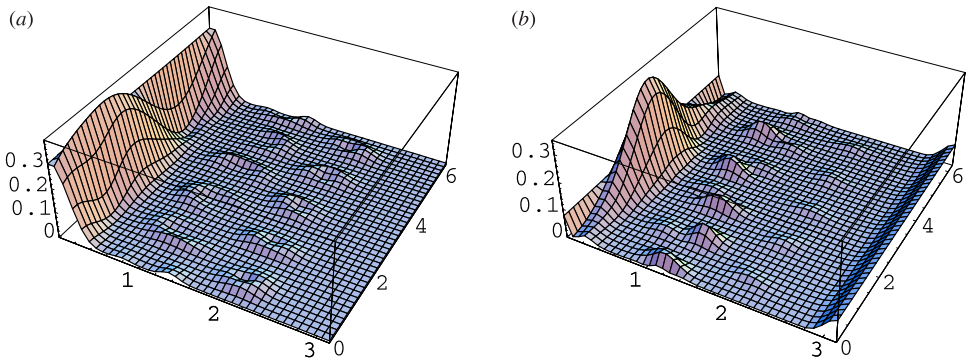

Figure 4. Time evolution of the Q-function for the coherent state $|\beta = 0.199, \phi = 0\rangle$: (*a*) $t = 1440\,000\hbar/\langle J \| T^{[6]} \| J \rangle$ and (*b*) $t = 80\,000\,000\hbar/\langle J \| T^{[6]} \| J \rangle$.

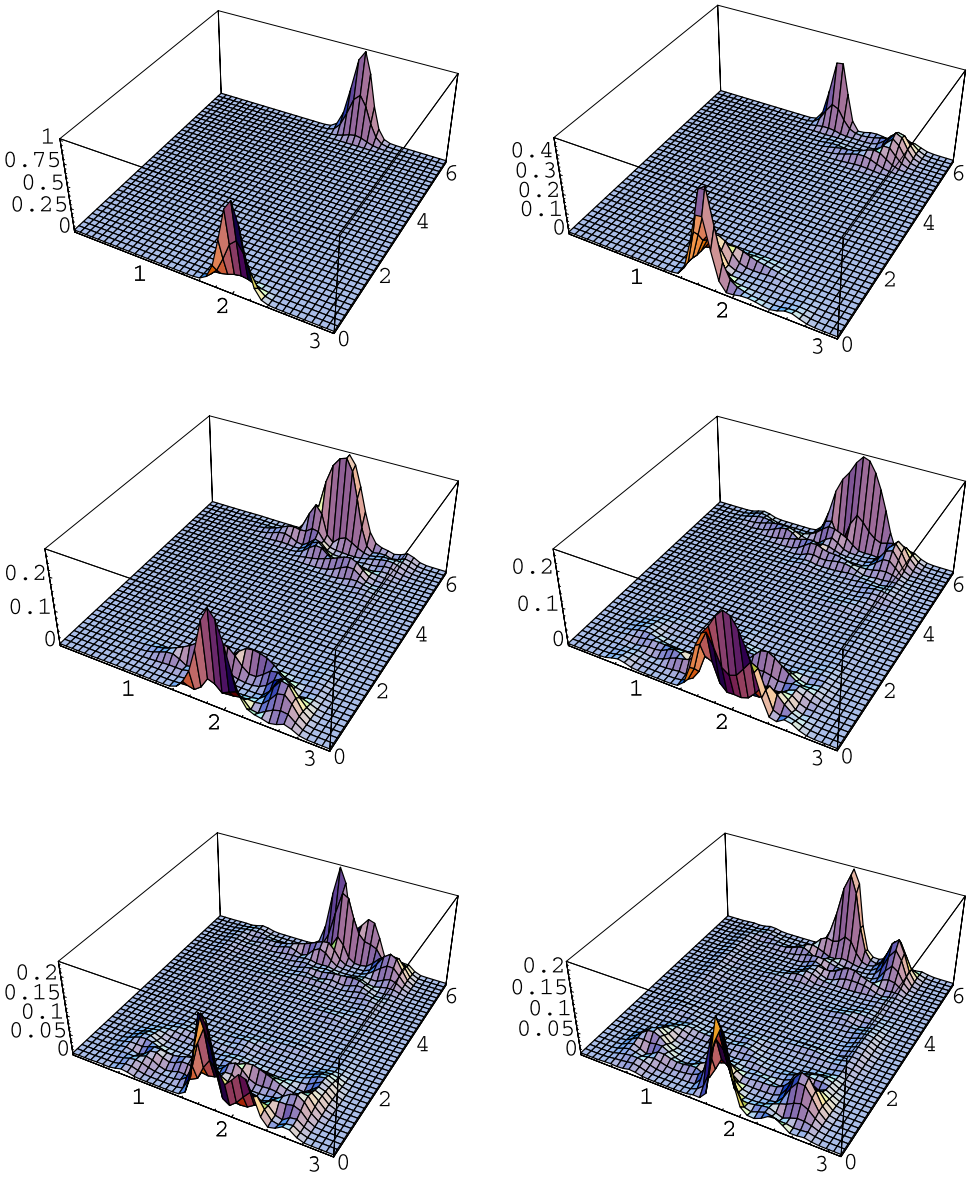

Figure 5. Time evolution of the Q-function for the coherent state $|\beta = 1.998, \phi = 0\rangle$: time steps in units of $t = 30\hbar/\langle J\|T^{[6]}\|J\rangle$. The plots are ordered from left to right and from top to bottom.

wavepacket and its corresponding classical dynamics on the associated 2-sphere which represents the classical phase space of the rotational degrees of freedom.

Let us consider a coherent state with $J = 60$ which is localized close to the north pole of the 2-sphere, with $\beta = 0.199$, $\phi = 0$ and with the mean energy $\langle \hat{H} - B\boldsymbol{J}^2\rangle/\langle J\|T^{[6]}\|J\rangle = 0.348$. The corresponding possible classical trajectories describe precessions of the body-fixed angular momentum around the 12 local maxima of the Hamiltonian of equation (1). One of these maxima is the north pole. Within a semiclassical framework the period of this precession determines the energy quantization in the neighbourhood of this mean energy. The quantum

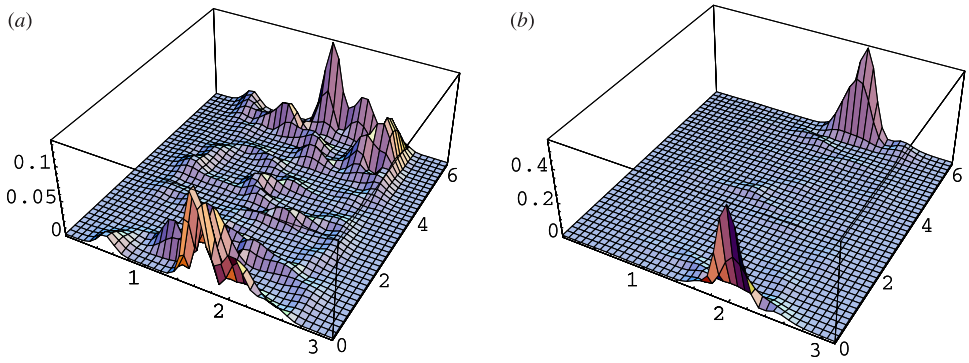

Figure 6. Time evolution of the Q-function for the coherent state $|\beta = 1.998, \phi = 0\rangle$: (*a*) $t = 40\,000\hbar/\langle J\|T^{[6]}\|J\rangle$ and (*b*) $t = 81\,470\hbar/\langle J\|T^{[6]}\|J\rangle$.

dynamics of the rotational degrees of freedom are summarized in figures 3 and 4. The sequence of Q-functions is given in time steps of magnitude $[40\hbar/\langle J\|T^{[6]}\|J\rangle]$ from top to bottom and from left to right. The initial stage of the time evolution of the wavepacket reflects the classical precession around the north pole. However, eventually the dispersion of the wavepacket leads to the characteristic scenario of fractional revivals [9–11]. The splitting of the original wavepacket around time $t = 80\hbar/\langle J\|T^{[6]}\|J\rangle$ into two parts is clearly visible in figure 3. This splitting takes place at one fourth of the revival time. The revival time T_R itself is defined by the relation

$$\frac{1}{2}\frac{\mathrm{d}^2E(n)}{\mathrm{d}n^2}T_R/\hbar = 2\pi. \tag{12}$$

For our purposes we may approximate the second derivative by the finite difference

$$\frac{\mathrm{d}^2E(n)}{\mathrm{d}n^2} = E(1) + E(3) - 2E(2) \tag{13}$$

with $E(1) = 0.557, E(2) = 0.362$ and $E(3) = 0.200$. The resulting revival time $T_R = 380\hbar/\langle J\|T^{[6]}\|J\rangle$ is consistent with figure 3.

The long-time behaviour of the rotational wavepacket is depicted in figure 4 for times $t = 1.44\times10^6\hbar/\langle J\|T^{[6]}\|J\rangle$ (*a*) and $80.00\times10^6\hbar/\langle J\|T^{[6]}\|J\rangle$ (*b*). These figures demonstrate that, in addition to revival phenomena, the long-time dynamics of the wavepacket is also dominated by tunnelling between the 12 possible classical trajectories which are associated with the mean energy and the angular momentum of the initial coherent state. As a result of this tunnelling maxima appear in the Q-function at time $t = 1.44\times10^6\hbar/\langle J\|T^{[6]}\|J\rangle$ (figure 4(*a*)) at the positions of the maxima of the classical Hamiltonian of equation (4). At even longer integration times, e.g. at $t = 80.00\times10^6\hbar/\langle J\|T^{[6]}\|J\rangle$, the wavepacket also tunnels to the south pole of the 2-sphere. The characteristic time scale on which these tunnelling phenomena take place is determined by the superfine-structure splittings of the multiplet depicted in figure 1. Within a semiclassical framework the magnitude of these splittings is determined by imaginary classical actions which characterize tunnelling through the energy barriers between classically accessible regions of phase space. The large magnitude of the characteristic tunnelling time originates from the large energy barriers which separate different classical trajectories.

The time evolution of an initial coherent state $|\beta = 1.998, \phi = 0\rangle$ is depicted in figures 5 and 6. The average energy of this coherent state is equal to the separatrix energy, i.e. $\langle\hat{H} - B/J^2\rangle/\langle J\|T^{[6]}\|J\rangle = -0.207$. At this particular energy the classical trajectories form

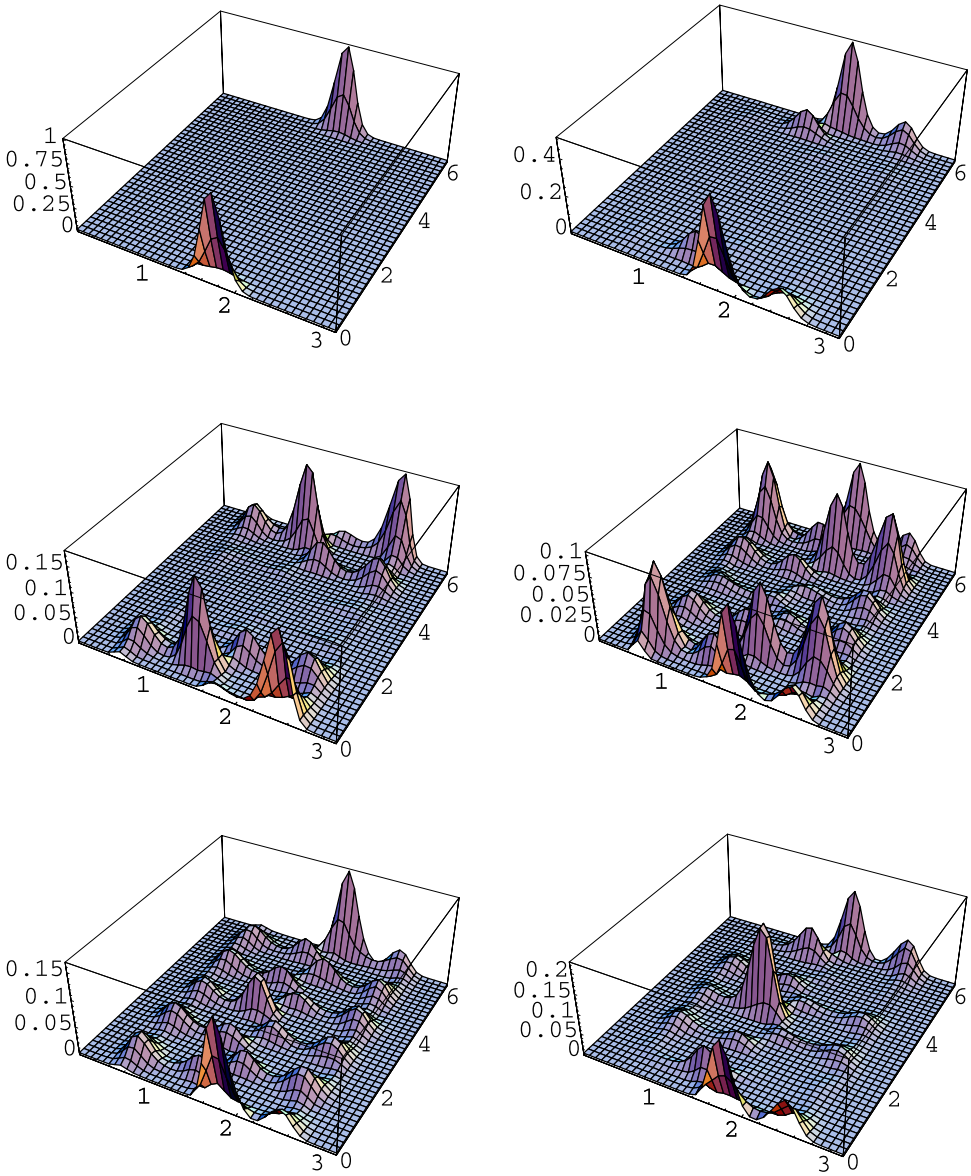

Figure 7. Time evolution of the Q-function for the coherent state $|\beta = 1.752, \phi = 0\rangle$: time steps in units of $t = 300\hbar/\langle J\|T^{[6]}\|J\rangle$. The plots are ordered from left to right and from top to bottom.

a network of closed orbits which extends over the 2-sphere. These classical orbits are formed by paths which connect all 30 unstable fixed points of the Hamiltonian of equation (4). The time evolution of the Q-function is shown in time steps of magnitude $[30\hbar/\langle J\|T^{[6]}\|J\rangle]$. It is apparent how the initially prepared wavepacket spreads on the 2-sphere along the classically accessible paths. The dynamics of this spreading resembles aspects of quantum mechanical tunnelling at the top of an energy barrier. The time evolution for longer times, i.e. for $t = 40\,000\hbar/\langle J\|T^{[6]}\|J\rangle$ figure 6(a) and for $t = 81\,470\hbar/\langle J\|T^{[6]}\|J\rangle$ figure 6(b) is shown in figure 6. At $t = 40\,000\hbar/\langle J\|T^{[6]}\|J\rangle$ the wavepacket is delocalized over the

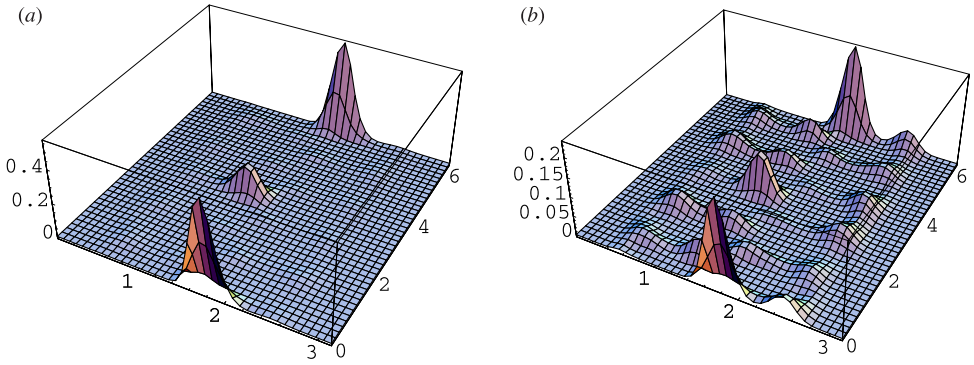

Figure 8. Time evolution of the Q-function for the coherent state $|\beta = 1.752, \phi = 0\rangle$: (*a*) $t = 50\,000\hbar/\langle J\|T^{[6]}\|J\rangle$ and (*b*) $t = 93\,000\hbar/\langle J\|T^{[6]}\|J\rangle$.

whole network of classical paths which extends over the 2-sphere. This spreading along this classical network of trajectories is accompanied by characteristic revival phenomena. At time $t = 81\,470\hbar/\langle J\|T^{[6]}\|J\rangle$, for example, the Q-function exhibits a complete revival.

The time evolution of a coherent state $|\beta = 1.752, \phi = 0\rangle$ is depicted in figures 7 and 8. The mean energy of this coherent state is $\langle\hat{H} - B\boldsymbol{J}^2\rangle/\langle J\|T^{[6]}\|J\rangle = -0.309$. Thus the initial coherent state is localized close to one of the 20 minima of the Hamiltonian of equation (4). The time evolution is shown in time steps of magnitude $[300\hbar/\langle J\|T^{[6]}\|J\rangle]$. For this particular energy the classical trajectories are closed orbits on the 2-sphere which are concentrated around the 20 minima of the Hamiltonian. As the energy barriers between two minima are much lower than the corresponding energy barriers between two maxima of the Hamiltonian (4) the characteristic time scale of tunnelling is much smaller than in the case considered in figures 3 and 4. The effects of tunnelling are apparent from figure 7. Eventually the wavepacket is concentrated in the neighbourhoods of all the 20 minima of the Hamiltonian (4). One also notices the revival of the wavepacket at $t = 4 \times 300\hbar/\langle J\|T^{[6]}\|J\rangle$. As a result of the characteristic revival phenomena at particular times the wavepacket may be localized also around some of these minima only thus forming various cat-like quantum states. Two such cases are depicted in figure 8 for times $t = 50\,000\hbar/\langle J\|T^{[6]}\|J\rangle$ (*a*) and for $t = 93\,000\hbar/\langle J\|T^{[6]}\|J\rangle$ (*b*). It is the non-trivial quantum rotational dynamics induced by the icosahedral symmetry of the rotational degrees of freedom which prepares this special type of cat-like state, which are localized in different regions of phase space.

4. Conclusions

The wavepacket dynamics of the rotational degrees of freedom of a C_{60} molecule in its electronic and vibrational ground state have been investigated. Due to the icosahedral symmetry of this ground state this dynamics exhibits a rich scenario of quantum coherence phenomena. For sufficiently short times the dynamics is dominated by the underlying classical dynamics in phase space. On longer time scales the dynamics is dominated by characteristic coherence phenomena such as fractional revivals, quantum tunnelling and the resulting appearance of cat-like states. The time scales on which these phenomena start to appear depend strongly on whether the initial quantum state is localized near a minimum, near a maximum or close to a saddle point of the relevant classical energy surface.

Acknowledgments

Financial support by the A von Humboldt foundation and by the Ministry of Education of the Czech Republic (MSM 210000018) for IJ is gratefully acknowledged. GA acknowledges support by the Deutsche Forschungsgemeinschaft within the SPP 'Zeitabhängige Phänomene in Quantensystemen der Physik und Chemie'. The authors would like to thank Professor A Zeilinger and Dr M Arndt for stimulating discussions.

References

[1] Berman P R 1997 *Atom Interferometry* (New York: Academic)
[2] Kroto H W and Walton D R M 1993 *The Fullerenes* (Cambridge: Cambridge University Press)
[3] Arndt M, Nairz O, Vos-Andreae J, Keller C, van der Zouw G and Zeilinger A 1999 *Nature* **401** 680
[4] Harter W G and Weeks D E 1989 *J. Chem. Phys.* **90** 4727
[5] Harter W G and Weeks D E 1986 *Chem. Phys. Lett.* **132** 387
[6] Edmonds A R 1957 *Angular Momentum in Quantum Mechanics* (Princeton, NJ: Princeton University Press)
[7] Perelomov A M 1972 *Commun. Math. Phys.* **26** 222
[8] Dowling J P, Agarwal G S and Schleich W P 1994 *Phys. Rev.* A **49** 4101
[9] Averbukh Sh I and Perelman N F 1989 *Phys. Lett.* A **139** 449
[10] Leichtle C, Averbukh I Sh and Schleich W P 1996 *Phys. Rev. Lett.* **77** 3999
[11] Jex I and Orlowski A 1994 *J. Mod. Opt.* **41** 2301